Science and Technology Indonesia
e-ISSN:2580-4391 *p*-ISSN:2580-4405
Vol. 9, No. 2, April 2024

Research Paper

Synthesis and Characterization of ZnO/Cellulose Acetate Composite and its Activity as Antibacterial Agent

Yemima Chellyne Khefanny[1], Charlena[1*], Sri Sugiarti[1]

[1]*Department of Chemistry FMIPA IPB University, IPB Campus, Dramaga, Bogor, 16680, Indonesia*
***Corresponding author**: charlena@apps.ipb.ac.id*

Abstract
Cellulose is an abundant natural polymer that can be applied in various fields. Cellulose has many types and derivatives, one of which is cellulose acetate. Cellulose can be obtained from various natural sources such as kepok banana peel. The α-cellulose content in kepok banana peel is high enough at 94% so that it can be utilized as a cellulose acetate raw material. Modification of cellulose acetate using antibacterial agents is needed, considering that cellulose does not have antibacterial properties. Metal oxide materials such as ZnO nanoparticles are used as antibacterial agents. This study added ZnO nanoparticles to cellulose acetate and tested its antibacterial activity. The characteristics of ZnO were analyzed by UV-Vis, PSA, and FTIR. The characteristics of cellulose acetate and composites were analyzed by FTIR and XRD. Antibacterial activity tests were performed on all samples. The results showed the band gap value of ZnO was 3.37 eV. The average size of ZnO nanoparticle distribution using PSA was 96.23 nm with an average PI value of 0.151. An indicator that the ZnO compound and cellulose acetate have been sucessfully mixed is the absorption band at wave number 488 cm^{-1}. A composite crystal size of 24.14 nm and a crystallinity percentage of 34.05% were found using XRD data. *S. aureus* bacteria are more inhibited by all evaluated substances antibacterial properties than *E. coli* germs. ZnO/Cellulose Acetate composite is categorized as strong inhibition, while ZnO nanoparticles are categorized as medium inhibition.

Keywords
Antibacterial, Cellulose Acetate, Composite, Nanoparticle ZnO

Received: 22 August 2023, Accepted: 18 January 2024
https://doi.org/10.26554/sti.2024.9.2.215-223

1. INTRODUCTION

Natural polymers, synthetic biopolymers, sugar-based biopolymers, and cellulosic biopolymers are the four different categories of biopolymers (Baranwal et al., 2022). Cellulose is an abundant and widespread biopolymer in nature with properties that are biocompatible, environmentally friendly because it is non-toxic, easily degradable, and renewable. Cellulose can be utilized in the industrial field in its pure form and its derivative products. One of the cellulose derivative products that are much needed by the industry is cellulose acetate. Cellulose acetate is cellulose in which an acetyl group has been added in place of the hydroxyl group. Because of its excellent physical and optical properties, cellulose acetate has a high market value and is frequently used as a membranes, photographic films, plastics, cigarette filters, fiber for textiles, and paper coatings.

Several plants are based on cellulosic sources such as banana peels, sweet potato peels, corn cobs, and other plants (Rahmatullah et al., 2022). Banana peels can be used as a source of raw materials for the manufacture of cellulose acetate because of its seasonal availability. Banana peel waste contains polymers such as lignin, cellulose, hemicellulose, and pectin. The α-cellulose content in kepok banana peel is quite high, which is 94% so it can be utilized as raw material for cellulose acetate.

Cellulose is a homo-polymer while chitosan is a hetero-polymer. While cellulose is not known to have antibacterial qualities, chitosan does since it can prevent pathogenic bacteria and rotting germs. The sensitivity of cellulose to bacteria is due to its typical porous structure and ability to maintain water content which makes it a perfect place for bacterial growth. Excessive growth of microorganisms on cellulose can cause hygiene and health problems for users of cellulose-based products and reduce the value of the product when used. Antibacterial finishing on cellulose is necessary to protect against bacteria. Nanotechnological antibacterial finishing uses nano-sized materials such as ZnO nano metal oxide.

Zinc oxide (ZnO) is the safest metal oxide compared to other metal oxides so it is widely used in industry as an antibacterial agent. Gold nanoparticles, bimetallic nanomaterials (Ag/Au, Ag/Pt), graphene-based materials, and metal oxide nanoparticles such as TiO_2, CuO, and SiO_2 have toxicity prob-

lems at the nanoscale so their use in humans is limited. ZnO is a biocompatible, biodegradable, and low toxicity substance (Herrera-Rivera et al., 2017). According to Jones et al. (2008), comparing ZnO to other metal oxide nanoparticles, *S. aureus* is more susceptible to its antimicrobial effects. Nanoparticles easily agglomerate at high calcination temperatures so this study added PVP surfactant as a capping agent.

The photocatalytic capabilities of metal oxide are linked to its antibacterial action. The photocatalytic process produces oxygen radicals that have and adverse effect on the growth of bacteria so that the structure of the cell membrane changes and the bacteria will die. The ZnO/Cellulose Acetate composite will combine the advantages of cellulose acetate and ZnO nanoparticles. ZnO powder can be combined with other materials with ease, but it is not easily formed into a tool or mold on its own. In contrast, cellulose can be molded into a tool due to its flexibility, but it lacks antibacterial properties. Combining ZnO and cellulose acetate will produce a composite that has good antibacterial activity and fluorescence, thus expanding the application of cellulose acetate and ZnO (Zhao et al., 2018). The combination of cellulose matrix and metal oxide nanoparticles is emerging as a very promising research field to develop new functional materials because of its benefits, which include affordability, ease of use, environmental friendliness, and functionality.

2. EXPERIMENTAL SECTION

2.1 Materials

The study's materials included were $ZnSO_4.7H_2O$ (Merck), NaOH (Merck), PVP (HIMEDIA), kepok banana peel, acetic anhydride (Merck), glacial acetic acid (Merck), sulfuric acid (Merck), and aquadest. The material for the UV-Vis test is 10% DMSO solvent from Merck. Materials for the antibacterial test were Muller Hinton Agar from Merck, DMSO 10%, Gram-positive bacteria *S. aureus* and Gram-negative bacteria *E. coli*. The characterization used a set of UV-Vis instruments (U-2800 spectrophotometer), a set of PSA instruments (SZ-100 HORIBA), a set of XRD instruments (XRD Empyrean Series 3), and a set of FTIR instruments (Shimadzu).

2.2 Methods

2.2.1 Synthesis of ZnO Nanoparticles (Ahmed et al., 2016)

ZnO nanoparticles were created by dissolving 15% PVP solution in 0.2 M $ZnSO_4.7H_2O$ solution while stirring continuosly for 25 minutes at 50°C. After two hours of stirring, a 0.4 M NaOH solution was added dropwise to the combined solution. To get rid of any remaining salt, the resultant precipitate was filtered and cleaned with distilled water so that $Zn(OH)_2$ and Na_2SO_4 precipitates were formed. After that, the white precipitate was dried for 3 hours at 120°C in an oven. In the final step, the product precipitate was calcined at 800°C in a furnace for 4 hours. The obtained samples were gathered at room temperature and stored in an airtight container.

2.2.2 Cellulose Acetate Synthesis

2.2.2.1 Preparation of Cellulose from Kepok Banana Peels

The preparation process of cellulose from kepok banana peel was carried out in 3 stages. The first stage is prepared ±20 kepok banana peels, then soaked in water to separate the dirt contained in the banana peel. In the second stage, the banana peels were cut and mashed into pulp and then put into 17.5% NaOH solution with 45°C heating for 1 hour. The material that does not dissolve in the solution is the main material to be obtained, namely α-cellulose. The third stage is the separation of α-cellulose from the solution using a paper filter. α-cellulose is washed with warm water at temperatures below 50°C. After performing all stages, the material obtained from the preparation was in the form of α-cellulose solids.

2.2.2.2 Synthesis

The cellulose acetate synthesis process was carried out in 4 stages, namely swelling, acetylation, hydrolysis, and purification. The swelling stage was carried out by dissolving 10 g α-cellulose into 100 mL glacial acetic acid for 1 hour at 45°C. The acetylation stage is done by adding 0.5 mL concentrated sulfuric acid and 50 mL acetic anhydride for 3 hours at 45°C. The hydrolysis stage which aims to stop the acetylation process is carried out by adding distilled water 25 mL and glacial acetic acid 50 mL heated at 50°C for 30 minutes. Then the purification stage is carried out by washing using distilled water until the pH is neutral. The result obtained is a white cellulose acetate precipitate. The precipitate was dried for 6 hours at 60-70°C in an oven.

2.2.3 Synthesis of ZnO/Cellulose Acetate Composite (Modification (Aly and Ahmed, 2021)

ZnO nanoparticles were mixed with synthetic cellulose acetate to create the ZnO/Cellulose Acetate composite. A total of 10 mL of cellulose acetate (b/v) solution (1:1) was mixed with 1 g of ZnO powder. The mixed solution was then sonicated for 2 hours to obtain a well-dispersed solution. After that, the mixture was filtered and again cleaned with distilled water. After that, the composite was dried for 4 hours at 60°C in an oven.

2.2.4 Cellulose Acetate Data Analysis

2.2.4.1 Determination of α-Cellulose Content (SNI 0444: 2009)

During the analysis, the temperature of water and sodium hydroxide was kept at 25°C ± 0.2°C. The weighing bottle and the sand funnel were heated to a constant weight of 105°C ± 5°C, cooled to room temperature in a desiccator, and then weighed with an accuracy of 0.5 mg. The moisture content of the sample was then determined. Both samples were weighed 1.5 g ± 0.1 g each with an accuracy of 0.1 mg. The sample was put into a 300 mL tall glass cup and 75 mL of 17.5% sodium hydroxide solution was added. The addition of the sodium hydroxide solution was timed. The pulp is then stirred until it is completely dispersed. Air bubbles in the pulp suspension

are avoided during the stirring process. The pulp attached to the stirring rod's end is cleaned once the pulp has scattered and the stirrer is raised. After adding the stirrer to a glass goblet, 25 mL of a 17.5% sodium hydroxide solution was used to wash it. This made a total of 100 mL of solution added to the pulp. Following the initial addition of sodium hydroxide solution, 100 mL of distilled water were added and agitated for 30 minutes. The goblet was left in the bath for a further half four, for a total extraction duration of roughly 60 minutes. The suspension was put into a masher funnel and swirled with a stir bar for 60 minutes. After discarding the first 10 to 20 mL of filtrate, approximately 100 mL of filtrate were collected and stored in a clean and dry flask. The pulp was not rinsed or washed with distilled water and care was taken that no bubbles passed through the pulp during filtration. A 250 mL flask was filled with 25 mL of filtrate and 10 mL of 0.5 N potassium dichromate solution. With caution, 50 mL of strong sulfuric acid was added while the flask was shaking. After 15 minutes of heating the solution (the temperature was heated at 125°C to 135°C), 50 mL of distilled water were added and the mixture was allowed to cool to room temperature. Following the addition of 2 to 4 drops of ferroin indicator, 0.1 N ferrous ammonium sulfate solution was titrated until the mixture turned purple. In order to conduct a blank titration, 12.5 mL of 17.5% sodium hydroxide solution and 12.5 mL of distilled water were added to the pulp filtrate. α-cellulose content is calculated by the following formula :

$$X = 100 - \frac{6.85(V_1 - V_2) \times N \times 20}{A \times W}$$

Where:
X = α-cellulose (%)
V_1 = titration volume of blank (mL)
V_2 = titration volume of pulp filtrate (mL)
N = normality of ferrous ammonium sulfate solution
A = volume of analyzed pulp filtrate (mL)
W = oven dry weight of pulp test sample (g)

2.2.4.2 Determination of Acetyl Content and Degree of Substitution

1 g of powdered synthesized cellulose acetate was added to an Erlenmeyer along with 40 mL of 75% (v/v) ethanol, and the mixture was heated for 30 minutes at 55°C in a water bath. Erlenmeyer was then taken out of the bath, 40 mL of 0.5 N NaOH was added, and the mixture was heated once again for 30 minutes at 55°C. Erlenmeyer was covered with aluminum foil and allowed to stand for 72 hours. Erlenmeyer added 2 drops of pp indicator and titrated with 0.5 N HCl (recorded the amount of HCl used) until the red color disappeared. Erlenmeyer was covered again with aluminum foil and allowed to stand for 24 hours to make NaOH diffuse. After that, titrated with 0.5 NaOH until a pink color hue forms. The same treatment for the blank but without the addition of cellulose acetate powder. The formula was used to calculate the acetyl content:

$$AC(\%) = [(D\text{-}C)Na + (A\text{-}B)Nb] \times \left(\frac{F}{W}\right)$$

The degree of substantiation is calculated using the formula :

$$DS = \frac{162 \times \left(\frac{\%acetyl}{43}\right)}{100 - \left(\frac{42}{43} \times \%acetyl\right)} \times 100\%$$

Where:
AC = acetyl content (%)
A = volume of NaOH used for sample titration (mL)
B = volume of NaOH used for blank titration (mL)
C = volume of HCl used for sample titration (mL)
D = volume of HCl used for blank titration (mL)
Na = Normality of HCl
Nb = Normality of NaOH
F = 4.305
W = sample weight

2.2.4.3 Water Content Analysis

Empty petri dishes were dried for 1 hour in an oven at 103°C, then cooled in a desiccator, then weighed (W_1). After that, 1 g of sample (W_2) was added, dried in an oven at 103°C for 2 hours, then cooled in a desiccator, and then weighed (W_3).

$$\text{Water content} = \frac{W_2 - W_3}{W_1} \times 100\%$$

2.2.4.4 Antibacterial Activity Test

The antibacterial activity test was conducted using the swab method. 15 mL of liquid MHA (Muller Hinton Agar) medium was put into a Petri dish. Using sterile cotton swabs, bacterial suspensions of *S. aureus* and *E. coli* were obtained and then aseptically streaked over the whole surface of the MHA media. Sterile disc paper containing the sample was placed on MHA agar media. Then incubated at 37°C for 1 day. The zone of inhibition formed around the disc is characterized by a clear zone and measured using a push-pull term.

3. RESULTS AND DISCUSSION

3.1 ZnO Nanoparticle

Synthesis of ZnO nanoparticles using $ZnSO_4.7H_2O$ precursor as zinc base material, NaOH precipitating agent, and distilled water as solvent. The mechanism of ZnO nanoparticle formation with $ZnSO_4.7H_2O$ precursor and NaOH precipitator is as follows (Ahmed et al., 2016):

$$2NaOH_{(s)} \rightarrow 2Na^+_{(aq)} + 2OH^-_{(aq)}$$

$$ZnSO_4.7H_2O_{(s)} \rightarrow Zn^{2+}_{(aq)} + SO^{2-}_{4\,(aq)} + 7H_2O$$

NaOH solution was dripped into $ZnSO_4.7H_2O$ solution with heating

$$Zn^{2+}_{(aq)} + 2OH^-_{(aq)} + xH_2O_{(aq)} \rightarrow Zn(OH)_2.xH_2O_{(s)}\downarrow$$

$$2Na^+ + SO_4^{2-} \rightarrow Na_2SO_4$$

$Zn(OH)_2$ was dried in an oven and calcined to produce ZnO powder

$$Zn(OH)_2.xH_2O_{(s)}\downarrow \rightarrow Zn(OH)_{2(s)} + xH_2O_{(g)}$$

$$Zn(OH)2_{(s)} \rightarrow ZnO_{(s)} + H_2O$$

The synthesis results produced ZnO nanoparticles in the form of white and dry powder with a yield of 53.3% (Figure 1). The calcination temperature used in this study is quite high at 800°C where according to Vasiljević et al. (2021), the higher the calcination temperature, the smaller the particle size. The calcination process can trigger high surface energy which will cause nanoparticle agglomeration. Agglomeration can be prevented by adding a capping agent to the nanoparticle synthesis. This study used a 15% polyvinyl pyrrolidone (PVP) surfactant as a capping agent.

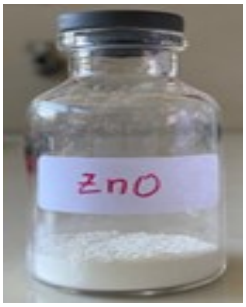

Figure 1. Synthesized ZnO Nanoparticles

3.2 Cellulose Acetate

Cellulose acetate synthesis using pisang kepok as a cellulose source. The calculation of ∝-cellulose content in this study refers to SNI 0444:2009 and obtained a pulp titration volume (V_2) of 29.2 mL, pulp filtrate volume (A) of 25 mL, sample dry weight (W) of 1.562 grams, blank titration volume (V_1) of 46.4 mL, and ferrous ammonium sulfate normality of 0.1 N. Based on these data, the ∝-cellulose content in kepok banana peel of 93.96% so it is in accordance with the literature. The water content of ∝-cellulose obtained was 3.64% which includes low moisture content. Low moisture content can prevent the growth of destructive microorganisms.

The ∝-cellulose powder was treated with glacial acetic acid for 1 hour. This pretreatment process aims to weaken the intramolecular forces in the form of hydrogen bonds that are quite strong in the lignocellulose chain. Furthermore, the acetylation process is carried out using acetic acid anhydride and concentrated sulfuric acid. After that, it is hydrolyzed using distilled water and glacial acetic acid. The mixture was then washed with distilled water and glacial acetic acid. The results obtained were filtered and dried, then crushed into powder. A white powder of cellulose acetate with a yield of 31.5% was obtained (Figure 2).

Analysis of acetyl content and degree of substitution aims to determine the type of cellulose acetate produced including monoacetate, diacetate, or triacetate. Calculation of acetyl content and degree of substitution of cellulose acetate obtained data of sample NaOH volume (A) of 21.5 mL, blank NaOH volume (B) of 10.7 mL, sample HCl volume (C) of 54 mL, blank HCl volume (D) of 63.8 mL, and sample weight (W) of 1.0034 grams. Based on these data, a degree of substitution of 2.9 and an acetyl content of 44.2% were obtained. From these results, the synthesized cellulose acetate belongs to cellulose triacetate. Cellulose triacetate can be used in the manufacture of fabrics and yarn wrapping.

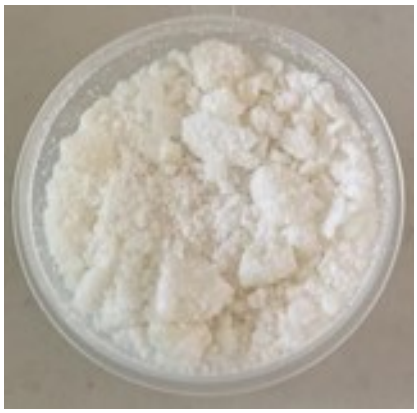

Figure 2. Cellulose Acetate Synthesized

3.3 Composite ZnO/Cellulose Acetate

Synthesize ZnO/Cellulose Acetate composite using the precipitation method. The precipitation method will increase the thermal stability of the composite. The composite was synthesized by inserting a nanofiller, namely ZnO nanoparticles, into a cellulose matrix, namely cellulose acetate. The filler serves to strengthen or harden the material of a composite while the matrix is responsible for binding the reinforcement together, holding the reinforcement to form a composite cluster. The result of the composite synthesis is a white powder with a yield of 60% (Figure 3).

3.4 UV-Vis Testing of ZnO Nanoparticle

Figure 4 is the UV-Vis absorbance curve of the synthesized ZnO sample with 15% PVP surfactant concentration. The absorbance value obtained is 4.66 at a wavelength of 368 nm which is in the UV-A absorption range. This result is not much different from the research Singh et al. (2023) that produced the excitonic absorption peak of ZnO nanoparticles at a wavelength of 367 nm. The energy band gap value is produced by applying the Tauc Plot method to the given spectrum data.

Figure 3. Synthesized ZnO/Cellulose Acetate Composite

The Tauc Plot method is done by making a graph of the relationship between $h\nu$ (energy) on the x-axis and $(\alpha h\nu)^2$ on the y-axis. The band gap value is determined by estimating the linear part of the curve of the relationship between $h\nu$ and $(\alpha h\nu)^2$ and from the extension of the linear line, the band gap energy value is obtained. The band gap result obtained is 3.37 eV (Figure 4). This is in accordance with Güngör and Gungor (2016) who stated that ZnO is a semiconductor material with a 3.37 eV broad band gap. Based on the band gap value obtained, it can be concluded that the synthesized ZnO includes semiconductor materials based on its energy gap value which ranges from 1 eV – 3 eV (Wibowo et al., 2020).

3.5 PSA Testing of ZnO Nanoparticle

A particle size analyzer (PSA) was used to determine the particle size analyzer. Particle size distribution analysis using ethanol as a dispersant. PSA testing of ZnO nanoparticles was carried out for 3 replicates. The average size distribution of ZnO nanoparticles is 96.23 nm with an average PI value of 0.151 (Table 1). Based on the average particle size results obtained, it can be seen that the synthesis results are good because the ZnO particle size is below 100 nm although the particle size is still large. This is thought to be because PVP, which acts as a capping agent, is able to reduce particle size and prevent aggregation so as to limit cluster growth so that the Zno clusters formed do not grow to a larger size and remain nano-sized. Zn^{2+} ions repel each other when in their ionic form due to the influence of similar charges. But when Zn atoms are reduced to Zno, their charge turns neutral, enabling them to approach and interact with one another through intermetallic bonds to form a cluster the size of a nanometer.

PSA determines the polydispersity index value in addition to particle size. The polydispersity index (PI) is a measure of sample heterogeneity by size (Mudalige et al., 2019). A particle has a polydispersity index (PI) range of 0.0 to 1.0. The particle size distribution is more homogenous the lower the PI value. A PI close to 0 indicates a uniform (homogeneous) particle distribution, while a PI higher than 0.5 indicates a heterogeneous particle distribution. Because the PI findings were less than 0.5, the results demonstrated that the dispersion of ZnO nanoparticles had a relatively uniform (homogeneous) particle distribution (Table 1) (Safithri et al., 2020).

3.6 FTIR Testing

Samples functional groups are examined using FTIR. FTIR uses infrared light with wave numbers 500-4000 cm^{-1}. Figure 5 shows the FTIR spectra of ZnO nanoparticles (a), cellulose acetate (b), and ZnO/Cellulose Acetate composite (c). The peaks at wave numbers 3378 cm^{-1}, 3438 cm^{-1}, and 3462 cm^{-1} correspond to the O−H stretch of H_2O, showing that the sample surface has absorbed water. Figure 5(c) shows a shift of higher wave numbers in the composite, demonstrating the water molecules high adhesion on the composite surface. The C=O stretch of the PVP molecule is shown by the peak at wave number 1636 cm^{-1} in the ZnO IR spectra. This indicates that PVP is still bound to the surface of ZnO particles (Gutul et al., 2014). The peak at wave number 1126 cm^{-1} corresponds to the C−N vibration of the PVP pyrrole ring (Koczkur et al., 2015). Because of atomic vibrations, metal oxides typically produce absorption bands in the fingerprint area, which is below 1000 cm^{-1} (Mahamuni et al., 2019). The absorption peak at wave number 488 cm^{-1} is associated with ZnO vibrational phonons (Kotresh et al., 2021).

In the IR spectra of cellulose acetate and ZnO/Cellulose Acetate composite, the absorption peaks at wave numbers 2938 cm^{-1} and 2921 cm^{-1} show the C−H stretch of the methyl group (CH_2) (Sudiarti et al., 2017). The absorption peaks of carbonyl groups (C=O) were marked at wave numbers 1754 cm^{-1} and 1740 cm^{-1} and ester groups (C−O) of acetyl groups at wave numbers 1058 cm^{-1} and 1045 cm^{-1}, respectively. This demonstrates the synthesis of cellulose acetate compounds with distinct peaks at wave numbers 1754 cm^{-1} and 1740 cm^{-1} as well as a reduction in OH group intensity brought on by acetyl group substitution. By comparing the IR spectra of ZnO and ZnO/Cellulose Acetate composite, the peak at wave number 1126 cm^{-1} is shifted to 1045 cm^{-1}. The peak shift can result from cellulose acetate and ZnO forming a hydrogen bond bridge (Padmalaya et al., 2019). The presence of ZnO was confirmed at wave number 488 cm^{-1} in the IR spectra of ZnO and ZnO/Cellulose Acetate composite. These results indicate that cellulose acetate was successfully bound to the composite surface.

3.7 XRD Testing

By comparing the strength of the diffraction peak and the value of the distance d (crystal plane) with standard data, X-ray diffraction is used to identify the crystal structure of a material. The ZnO nanoparticles X-ray diffraction pattern is displayed in Figure 6(a). ZnO nanoparticles show diffraction peaks with high intensity at angles (2θ) of 31.740° (100), 34.361° (002), and 36.194° (101). Other peaks with lower intensity are located at 47.487° (102), 56.603° (110), 62.800° (103), 66.331° (200), 67.891° (112) and 69.017° (201). These diffraction peaks show the diffraction peaks of the hexagonal wurtzite crystal structure which corresponds to the JCPDS standard no. 36-

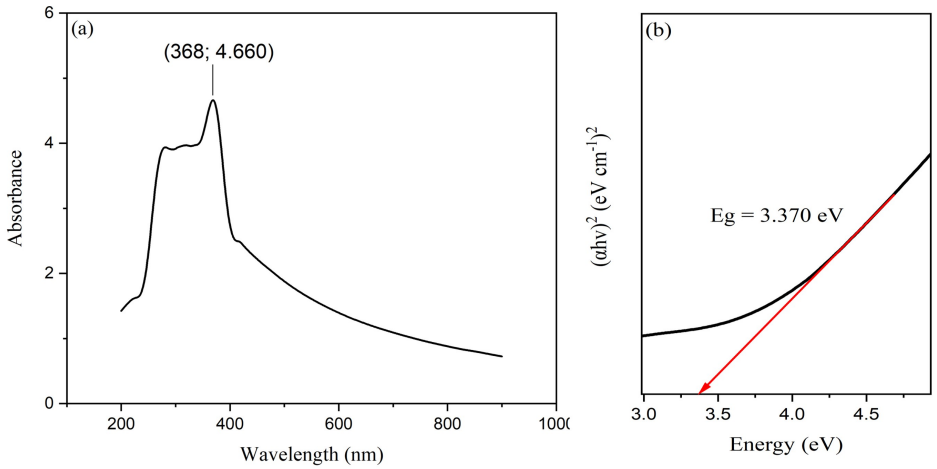

Figure 4. UV-Vis Spectrum (a) and Band Gap Energy (b) of ZnO Nanoparticles

Table 1. ZnO Particle Size Distribution

ZnO Particle Size (nm)			Average Size of ZnO (nm)	Polydispersity Index (PI)			Average of PI
1	2	3		1	2	3	
98.1	94.2	96.4	96.23	0.071	0.215	0.169	0.151

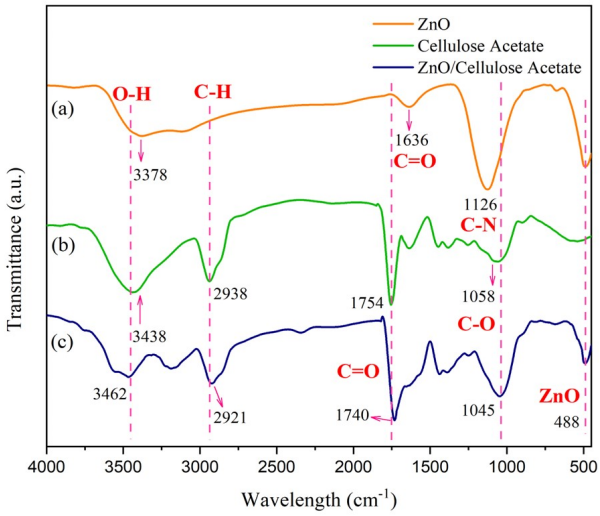

Figure 5. FTIR Spectra of ZnO Nanoparticles (a), Cellulose Acetate (b), and ZnO/Cellulose Acetate Composite (c)

1451 with values a = b = 3.249 and c = 5.206 (Chauhan et al., 2017). Strong and narrow diffraction peaks are found, which suggests that the ZnO nanoparticles have good crystallinity (Kotresh et al., 2021). The Debye Scherrer equation is used to find the crystal size, or ACS (Apparent Crystal Size), and ZnO nanoparticles have an average crystal size of 34.85 nm and a crystallinity of 72.7%.

Figure 6(b) shows the X-ray diffraction pattern of cellulose acetate from kepok banana peel. Cellulose acetate shows intensity at 2θ = 22.29°. The cellulose structure shown by the diffraction peak at 2θ around 20-22° is characteristic of native cellulose or often called cellulose I. The average size of cellulose acetate crystals was obtained as 29.99 nm with a crystallinity index of 57.75%.

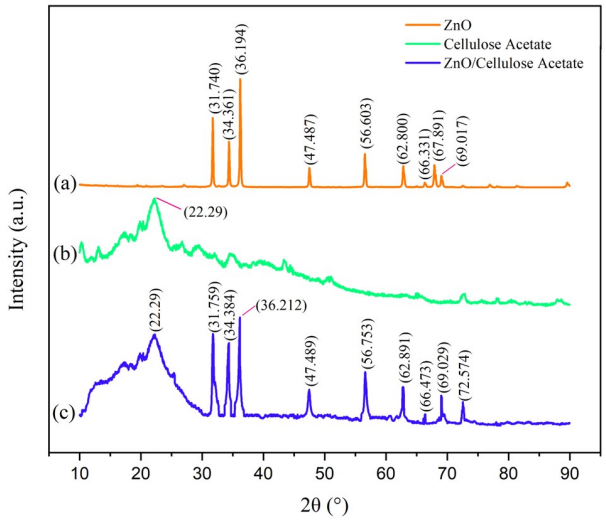

Figure 6. XRD Pattern of ZnO Nanoparticles (a), Cellulose Acetate (b), and ZnO/Cellulose Acetate Composite (c)

Figure 6(c) shows the X-ray diffraction pattern of ZnO/Cellulose Acetate composite. The XRD results show the effect

of mixing the compound in the form of ZnO on cellulose acetate. The characteristic peak of cellulose acetate shows a diffraction peak at $2\theta = 22.29°$. The characteristic peak of ZnO shows a diffraction peak with high intensity at angles 31.759° (100), 34.384° (002), and 36.212° (101) which corresponds to JCPDS no. 36-1451 which is a hexagonal wurtzite structure. Figure 6 shows that the ZnO/Cellulose Acetate composite peak shows a slight shift towards higher angles compared to pure ZnO nanoparticles. This is because the addition of ZnO into the cellulose matrix causes lattice distortion which also affects the size of the composite crystal. The crystal field will shrink after the addition of ZnO due to the radius of the Zn^{2+} atom and will result in variations in crystal size (Padmalaya et al., 2019). The average size of the composite crystal was obtained as 24.14 nm with a crystallinity index of 34.05%.

3.8 Antibacterial Activity

Using Gram-positive and Gram-negative bacteria, respectively, *S. aureus* and *E. coli*, ZnO nanoparticles and manufactured composites were tested for their antibacterial activities. Testing includes Gram positive and Gram negative bacteria because these two species have different levels of resistance to antibacterial agents. The test was carried out by evaluating the width of the clear zone that occurred on the bacteria type media after surface contact with paper disks that had previously been moistened with a colloidal solution of ZnO nanoparticles and composites with DMSO solvent. The antibacterial activity test using DMSO solvent is done because the solvent acts as an antibacterial standard so that the solvent does not affect the results of the ZnO nanoparticle antibacterial activity test (Kareem et al., 2018).

The test results showed that the ZnO nanoparticle solution and ZnO/Cellulose Acetate composite exhibited substantial antibacterial activity against *S. aureus* and *E. coli* bacteria with the formation of clear zones on agar media containing these bacteria (Figure 7). The size of the clear zone indicates the strength of inhibition of the test sample. The wider the clear zone formed, the stronger the inhibition of the compound against bacterial growth.

The ZnO/Cellulose Acetate composite exhibited superior antibacterial activity in comparison to ZnO, as demonstrated by the outcomes of antibacterial testing. The ZnO/Cellulose Acetate inhibition zone against *S. aureus* had an average width of 13.45 mm, indicating a substantial level of inhibition. The ZnO/Cellulose Acetate inhibition zone against *E. coli* had a mean width of 11.75 mm, indicating a substantial level of inhibition. ZnO's inhibition zone against *S. aureus* had a mean width of 10.36 mm, indicating a moderate level of inhibition. The ZnO inhibition zone's average width against *E. coli* was 9.67 mm, indicating a moderate level of inhibition. Regardless of the source or amount of cellulose in the ZnO/Cellulose Acetate composite, the higher the percentage of ZnO incorporation, the better the antibacterial activity of the composite can be produced.

Gram-positive bacteria (*S. aureus*) are more inhibited by both composite and ZnO samples than by Gram-negative bacteria (*E. coli*), according to the results of the antibacterial activity test. The effect of this antibacterial activity may be due to the difference in the structure of the bacterial cell membrane. Gram-positive bacteria are more easily destroyed due to their thicker peptidoglycan coating, because the layer is able to absorb antibacterials, antibiotics, or other cleaning products. In contrast, Gram-negative bacteria have a cell wall made up of an outer membrane around a thin layer of peptidoglycan. The distinctive structure of the multilayered outer membrane of Gram-negative bacteria can prevent some antibacterial agents from entering the cell. Gram-negative bacteria are better protected from certain physical attacks because they do not absorb foreign materials or materials that surround them (Breijyeh et al., 2020). Despite having a thin peptidoglycan layer, the presence of a multilayered membrane allows Gram-negative bacteria to control, sequester or even eliminate threats to the membrane before they reach the interior of the cell itself. Therefore, it is important to make sure that the method used can pierce the thick peptidoglycan coating of Gram-positive bacteria in order to decrease antibacterial activity (Ślusarz et al., 2014).

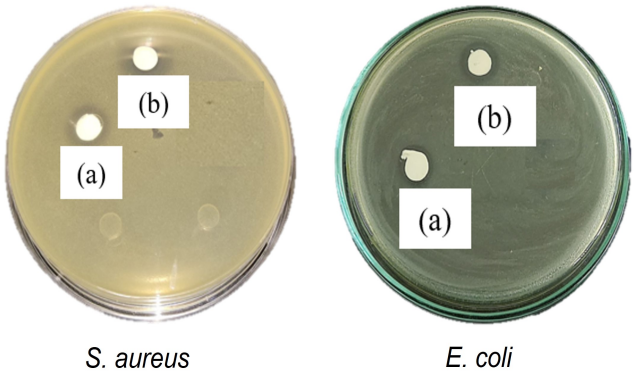

Figure 7. Inhibition Zone of ZnO Nanoparticles (a) and ZnO/Cellulose Acetate Composite (b) on Gram Positive *S. aureus* and Gram Negative *E. coli* Bacteria

Reactive species triggered by UV and visible light, such as superoxide, hydrogen peroxide, and hydroxyl, develop on the surface of ZnO and contribute to the antibacterial mechanism of ZnO/Cellulose composites (Jiang et al., 2020). Numerous scientists have hypothesized that the primary factor preventing bacterial growth on ZnO is H_2O_2 on its surface. During a redox reaction, H_2O_2 takes electrons from other reactants and gains them to become reduced. It is a strong oxidant of proteins, lipids, and nucleic acids that produces large amounts of hydroxyl radicals. As a result, it is able to interact with the macromolecular parts of microbes. The reaction of H_2O_2 formation is as follows (Zhao et al., 2018):

$$\text{ZnO/Cellulose Acetate} + h\nu\ (\lambda < 388\ \text{nm}) \rightarrow e^- + h^+$$
$$H_2O + h^+ \rightarrow H^+ + HO^\bullet$$

$O_2 + e^- \rightarrow O_2^{\bullet -}$

$O_2^{\bullet -} + H^+ \rightarrow HO_2^{\bullet}$

$HO_2^{\bullet} + e6- \rightarrow HO_2^-$

$HO_2^- + H^+ \rightarrow H_2O_2$

The results in this study show that there is an effect of ZnO metal oxide compounds on antibacterial activity, even though the compounds are composited in a cellulose matrix. Because it is able to limit bacterial development without releasing antibacterial chemicals into the environment, cellulose containing metal oxide can be classified as a passive antibacterial substance. Metal oxide compounds are able to disrupt the integrity of the bacterial cell wall, can cause lysis, and cell death. Nanoparticle size is one of the main factors affecting antibacterial activity. Small-sized nanoparticles show more antibacterial potential than larger nanoparticle sizes (Khandelwal et al., 2014). Smaller nanoparticle sizes favor the ease of passing through bacterial cell walls and disrupting bacterial metabolic pathways by affecting the shape and function of cell membranes which can lead to mitochondrial dysfunction, DNA damage, and bacterial death (Maślana et al., 2021). This is evident from the size comparison of ZnO nanoparticles with ZnO/Cellulose Acetate composites. From the XRD data, the size of the ZnO/Cellulose Acetate composite is smaller than the size of ZnO. It is clear that antibacterial activity increases with decreasing particle size (Yamamoto, 2001).

4. CONCLUSIONS

This research successfully synthesized ZnO nanoparticles, cellulose acetate, and ZnO/Cellulose Acetate composite. ZnO nanoparticles are used as antibacterial agents. Based on the results of the antibacterial activity test, it is shown that there is an effect of ZnO nanoparticles added to cellulose acetate. The antibacterial activity of ZnO nanoparticles is categorized as moderate inhibition, while the ZnO/Cellulose Acetate composite is categorized as strong inhibition. Both ZnO and the composite had a larger zone of inhibition against *S. aureus* bacteria than *E. coli*. The synthesized cellulose acetate belongs to the triacetate cellulose type according to the results of the degree of substitution and acetyl content, which can potentially be applied in the manufacture of fabrics and yarn wrapping.

5. ACKNOWLEDGEMENT

We would like to express our gratitude to the managers and instructors at IPB University's Laboratory of Inorganic Chemistry for helping to establish this research.

REFERENCES

Ahmed, M., M. Abd-Elhamid, A. Sarhan, and A. Hassan (2016). Preparation and Characterization of ZnO Nanoparticles by Simple Precipitation Method. *International Journal of Science, Engineering and Technology*, **4**(3); 507–512

Aly, A. A. and M. Ahmed (2021). Nanofibers of Cellulose Acetate Containing ZnO Nanoparticles/Graphene Oxide for Wound Healing Applications. *International Journal of Pharmaceutics*, **598**; 120325

Baranwal, J., B. Barse, A. Fais, G. L. Delogu, and A. Kumar (2022). Biopolymer: A Sustainable Material for Food and Medical Applications. *Polymers*, **14**(5); 983

Breijyeh, Z., B. Jubeh, and R. Karaman (2020). Resistance of Gram-Negative Bacteria to Current Antibacterial Agents and Approaches to Resolve It. *Molecules*, **25**(6); 1340

Chauhan, J., N. Shrivastav, A. Dugaya, and D. Pandey (2017). Synthesis and Characterization of Ni and Cu Doped ZnO. *MOJ Polymer Science*, **1**(1); 26–34

Güngör, E. and T. Gungor (2016). Influence of Aluminum Concentration on the Electrical and Optical Properties of ZnO Thin Films. *Journal of the Turkish Chemical Society Section A: Chemistry*, **3**(3); 453–462

Gutul, T., E. Rusu, N. Condur, V. Ursaki, E. Goncearenco, and P. Vlazan (2014). Preparation of Poly (N-Vinylpyrrolidone)-Stabilized ZnO Colloid Nanoparticles. *Beilstein Journal of Nanotechnology*, **5**(1); 402–406

Herrera-Rivera, R., M. Olvera, and A. Maldonado (2017). Synthesis of ZnO Nanopowders by the Homogeneous Precipitation Method: Use of Taguchi's Method for Analyzing the Effect of Different Variables. *Journal of Nanomaterials*, **2017**; 1–9

Jiang, S., K. Lin, and M. Cai (2020). ZnO Nanomaterials: Current Advancements in Antibacterial Mechanisms and Applications. *Frontiers in Chemistry*, **8**; 580

Jones, N., B. Ray, K. T. Ranjit, and A. C. Manna (2008). Antibacterial Activity of ZnO Nanoparticle Suspensions on a Broad Spectrum of Microorganisms. *FEMS Microbiology Letters*, **279**(1); 71–76

Kareem, A., M. Al Maamori, and S. N. AL-Thomir (2018). Preparation and Characterization of Antimicrobial PVA/ZnO Nanocomposite for Biomaterial Applications. *Journal of University of Babylon for Engineering Sciences*, **26**(2); 286–294

Khandelwal, N., G. Kaur, N. Kumar, and A. Tiwari (2014). Application of Silver Nanoparticles in Viral Inhibition: A New Hope for Antivirals. *Digest Journal of Nanomaterials & Biostructures (DJNB)*, **9**(1); 175–186

Koczkur, K. M., S. Mourdikoudis, L. Polavarapu, and S. E. Skrabalak (2015). Polyvinylpyrrolidone (PVP) in Nanoparticle Synthesis. *Dalton Transactions*, **44**(41); 17883–17905

Kotresh, M., M. Patil, and S. R. Inamdar (2021). Reaction Temperature Based Synthesis of ZnO Nanoparticles Using Co-Precipitation Method: Detailed Structural and Optical Characterization. *Optik*, **243**; 167506

Mahamuni, P. P., P. M. Patil, M. J. Dhanavade, M. V. Badiger, P. G. Shadija, A. C. Lokhande, and R. A. Bohara (2019). Synthesis and Characterization of Zinc Oxide Nanoparticles by Using Polyol Chemistry for their Antimicrobial and

Antibiofilm Activity. *Biochemistry and Biophysics Reports*, **17**; 71–80

Maślana, K., A. Żywicka, K. Wenelska, and E. Mijowska (2021). Boosting of Antibacterial Performance of Cellulose Based Paper Sheet Via TiO_2 Nanoparticles. *International Journal of Molecular Sciences*, **22**(3); 1451

Mudalige, T., H. Qu, D. Van Haute, S. M. Ansar, A. Paredes, and T. Ingle (2019). Characterization of Nanomaterials: Tools and Challenges. *Nanomaterials for Food Applications*; 313–353

Padmalaya, G., B. Sreeja, P. Dinesh Kumar, S. Radha, V. Poornima, M. Arivanandan, S. Shrestha, and T. Uma (2019). A Facile Synthesis of Cellulose Acetate Functionalized Zinc Oxide Nanocomposite for Electrochemical Sensing of Cadmium Ions. *Journal of Inorganic and Organometallic Polymers and Materials*, **29**; 989–999

Rahmatullah, R. W. Putri, M. Rendana, U. Waluyo, and T. Andrianto (2022). Effect of Plasticizer and Concentration on Characteristics of Bioplastic Based on Cellulose Acetate from Kapok (*Ceiba pentandra*) Fiber. *Science and Technology Indonesia*, **7**(1); 73–83

Safithri, M., S. Indariani, and R. Yuliani (2020). Effect of Microencapsulation Techniques on Physical and Chemical Characteristics of Functional Beverage Based on Red Betel Leaf Extract (*Piper crocatum*). *Jurnal Kimia Sains Dan Aplikasi*, **23**(8); 276–282

Singh, K., Nancy, M. Bhattu, G. Singh, N. M. Mubarak, and J. Singh (2023). Light-Absorption-Driven Photocatalysis and Antimicrobial Potential of PVP-Capped Zinc Oxide Nanoparticles. *Scientific Reports*, **13**(1); 13886

Ślusarz, R., M. Szulc, and J. Madaj (2014). Molecular Modeling of Gram-Positive Bacteria Peptidoglycan Layer, Selected Glycopeptide Antibiotics and Vancomycin Derivatives Modified with Sugar Moieties. *Carbohydrate Research*, **389**; 154–164

Sudiarti, T., D. Wahyuningrum, B. Bundjali, and I. M. Arcana (2017). Mechanical Strength and Ionic Conductivity of Polymer Electrolyte Membranes Prepared from Cellulose Acetate-Lithium Perchlorate. In *IOP Conference Series: Materials Science and Engineering*, volume 223. IOP Publishing, page 012052

Vasiljević, Z. Ž., M. P. Dojčinović, J. D. Vujančević, M. Spreitzer, J. Kovač, D. Bartolić, S. Marković, I. Janković-Častvan, N. B. Tadić, and M. V. Nikolić (2021). Exploring the Impact of Calcination Parameters on the Crystal Structure, Morphology, and Optical Properties of Electrospun Fe_2TiO_5 Nanofibers. *RSC Advances*, **11**(51); 32358–32368

Wibowo, A., M. A. Marsudi, M. I. Amal, M. B. Ananda, R. Stephanie, H. Ardy, and L. J. Diguna (2020). ZnO Nanostructured Materials for Emerging Solar Cell Applications. *RSC Advances*, **10**(70); 42838–42859

Yamamoto, O. (2001). Influence of Particle Size on the Antibacterial Activity of Zinc Oxide. *International Journal of Inorganic Materials*, **3**(7); 643–646

Zhao, S. W., C. R. Guo, Y. Z. Hu, Y. R. Guo, and Q. J. Pan (2018). The Preparation and Antibacterial Activity of Cellulose/ZnO Composite: A Review. *Open Chemistry*, **16**(1); 9–20

